Hindawi
Geofluids
Volume 2023, Article ID 8936092, 16 pages
https://doi.org/10.1155/2023/8936092

Research Article

Temperature Field Study of Offshore Heavy Oil Wellbore with Coiled Tubing Gas Lift-Assisted Lifting

Kechao Gao,[1] Qibin Zhao,[2] Xinghua Zhang,[1] Suogui Shang,[1] Lijun Guan,[3] Jizhi Li,[3] Na Xu,[4] Dagui Cao,[5] Liang Tao,[5] Hongxing Yuan,[6] and Yonghai Gao[6]

[1]*Tianjin Branch of CNOOC (China), Limited, Tianjin 300459, China*
[2]*CNOOC (China) Limited, Beijing 100010, China*
[3]*Shenzhen Branch, CNOOC (China) Co., Ltd., Shenzhen 518000, China*
[4]*Research Institute of Oil Production Engineering, PetroChina Daqing Oilfield Limited Company, Daqing 163453, China*
[5]*COSL-EXPRO Testing Services (Tianjin) Co., Ltd., Tianjin 300457, China*
[6]*School of Petroleum Engineering, China University of Petroleum (East China), Qingdao 266580, China*

Correspondence should be addressed to Yonghai Gao; upcgaoyh@163.com

Received 31 August 2023; Revised 18 October 2023; Accepted 5 December 2023; Published 18 December 2023

Academic Editor: Tianshou Ma

Offshore heavy oil resources are abundant, but they have greater difficulty and higher costs compared to onshore extraction. When crude oil flows through the seawater section, the temperature of the crude oil decreases faster, making it susceptible to solidification in the wellbore and resulting in lower well production. The cooling of crude oil becomes more pronounced in deep-water wellbore. However, the injection of low-temperature gas will have a cooling effect on the formation production fluid, which will have a negative effect. The model analyzes the effects of coiled tubing running depth, gas injection temperature, gas injection volume, coiled tubing diameter, and crude oil production on the temperature distribution of heavy oil in deep-water and shallow water wellbores. We propose recommendations for the selection of each parameter for deep and shallow water environments by analyzing and summarizing the laws.

1. Introduction

As conventional oil reservoirs continue to be developed, unconventional energy sources are becoming an important direction for exploration. Heavy oil has a pivotal role in global oil resources [1, 2]. Although marine heavy oil resources are abundant, but due to the economic costs, platform space, and environmental requirements and other conditions, the conventional method of extracting onshore heavy oil cannot be applied to offshore [3]. At present, offshore heavy oil is usually lifted by artificial lifting processes such as electric submersible pump, jet pump, screw pump, and gas lift. The oilfield selects the appropriate lifting process based on the specific formation conditions and fluid properties.

The coiled tubing gas lift heavy oil process has the characteristics of high economic benefits, simple and reliable construction, free control of the depth of descent, and less damage to the reservoir than other processes [4]. However, the process also has certain limitations. Field practice shows the cooling effect of mixing crude oil with low-temperature injection gas when using coiled tubing for gas lift. This will make the viscosity of heavy oil increase, leading to difficulties in draining the fluid, and cannot truly evaluate the production capacity. Therefore, it is of great practical significance to study the temperature field of offshore heavy oil wellbore with the assisted lift of coiled tubing gas lift. In this paper, we study the optimized design of coiled oil tubing gas lift process parameters to provide suggestions and guidance for field construction.

Temperature is one of the most critical parameters for evaluating the flowability of heavy oil, so it is especially important to study the temperature field of coiled tubing gas lift wellbore. Many experts and scholars have studied the wellbore temperature field. Some scholars propose a method to calculate the two-phase flow temperature by considering the heat conduction and convective heat transfer between the formation and the wellbore as well as the diffusion equation [5–7]. The analytical solutions for the transient and steady-state temperature fields are given separately, and the accuracy of the model is verified by comparing the results of the model calculations with the field example well data. [8] presented a semianalytic solution for the wellbore temperature profile, which directly transforms the isothermal flow model into a nonisothermal flow model using the reservoir continuity equation and the momentum conservation equation. They also designed the program using the model, which not only couples the reservoir to the wellbore but also improves the computational efficiency and is suitable for the simulation of conventional thermal reservoirs. [9] developed a mathematical model for the coupled temperature-pressure flow of fluid single-phase transient in the tubular column during gas well production. The pressure and temperature distribution patterns of gas in the tubular column during gas well production were obtained using the model, and the effect of production on temperature and pressure distribution was analyzed. The comparison of the field-measured data and the model calculation results shows that the coupling model has high accuracy. [10] established an improved thermal model for deep-water gas wellbore temperature prediction based on the proposed method for calculating the annular convective heat transfer coefficient of non-Newtonian fluids and the heat transfer model for annular mist flow in oil tubing. The model fits well with the measured data of deep-water gas wells, and the model prediction error is within 10%. The current wellbore temperature field is mainly studied for pure phases (gas and liquid) and gas and liquid phases alone. In contrast, the coexistence of the pure gas phase and the gas-liquid phase, which has the characteristics of a coiled tubing gas lift process, has rarely been studied.

For the development of offshore heavy oil, the use of appropriate artificial lifting methods will help to increase its production and realistically evaluate its capacity. The temperature distribution of different lifting processes has been studied in many articles.

[11] established and solved the mathematical model of the tubing electric heating viscosity reduction and lifting process based on the basic theory of heat transfer. They used the model to establish the relationship between pumping lift energy consumption and wellbore temperature field, which laid the foundation for optimizing electric heating power. [12] derived a model based on the law of energy conservation for predicting the wellbore temperature distribution during the extraction of heavy oil added from the annulus with light oil. Their calculated results using the temperature model were compared with the measured data, and the agreement was good. Finally, a sensitivity analysis was performed using the model, and the main factors affecting the temperature distribution were discussed. [13] developed a coupled pressure and temperature model based on the laws of conservation of mass, momentum, and energy, in which the heat transfer parameters were calculated using the Hasan-Kabir method, and the pressure drop was calculated using the Hagedorn-Brown method. The calculation results show that the requirements cannot be met by using only electric heating or light oil blending technology. In combination with electric heating technology, the amount of light oil can be reduced. In order to investigate whether the heat dissipation of the electric submersible pump has an impact on the stability of the wellbore, [14] modeled the transient wellbore temperature with full consideration of the heat dissipation of the electric submersible pump motor, pump, and cable. The calculation results of the model were compared with the measurement results of the field sensors, and the results showed that the model has good accuracy. [15] conducted an experimental study on annular injection of light oil-assisted heavy oil gas lift and established a coupled pressure-temperature model for annular injection of light oil gas lift wellbore using experimental results and basic theory of heat transfer. Model calculations show that the use of gas lift with diluted oil injection technology can significantly increase the capacity of heavy oil wells. Based on the law of energy conservation, [16] developed a wellbore temperature calculation model for lifting heavy oil using the jet pumping process, which includes the analytical solution of tubing and annulus temperature distribution. Finally, the model was validated using data from one well in the Tahe oilfield in China, and the results showed that the method matched well with the field data set. At present, the research objects of the temperature field of heavy oil are mainly electric heating, electric submersible pump, gas lift, blending light oil and jet pump, etc. The temperature field research for coiled tubing gas lift process has not been reported.

The process of coiled tubing gas lift is to inject compressed gas from the coiled tubing after the well is lowered into the coiled tubing and then discharged through the bottom of the coiled tubing, and the oil production fluid along with the gas flows from the annulus between the tubing and the coiled tubing from the bottom to the wellhead [17]. In this study, according to the process characteristics of coiled oil pipe gas lift, a temperature calculation model with pure gas phase inside the coiled oil pipe and gas-liquid phase outside the coiled oil pipe is established. The effects of temperature and pressure on the physical parameters are considered to make the calculation results more accurate. Using the established model, this paper analyzes the influence law of coiled tubing running depth, gas injection temperature, gas injection volume, coiled tubing diameter, and crude oil production on wellbore temperature distribution, which provides some theoretical guidance for offshore heavy oil testing and production.

2. Calculation Model for Wellbore Temperature of Coiled Tubing Gas Lift

2.1. Model Assumptions. The temperature of seawater remains almost constant throughout the entire process due to its ability to flow, while the temperature of the formation changes. Due to the flow of fluids, the radial heat transfer in the wellbore is much greater than the axial heat transfer. The physical properties of fluids are influenced by temperature and pressure, and flow friction also generates heat. Therefore, we can make the following assumptions.

(1) From the wellhead to above the mudline, the wellbore and seawater are regarded as steady-state heat transfer; below the mudline to the formation, the wellbore to the outer wall of the cement ring is considered as steady-state heat transfer, and the outer wall of the cement ring to the formation is considered as unsteady-state heat transfer

(2) The thermophysical properties of wellbore fluids are influenced by pressure and temperature

(3) Considering only the radial heat transfer and ignoring the heat transfer along the axial direction of the wellbore

(4) Considering the heat generated by friction between heavy oil flow and pipe wall

2.2. Temperature Distribution in Coiled Tubing Gas Lift Wellbore. The coiled tubing gas lift considers the Joule-Thompsoon effect generated by the expansion and compression of gas during wellbore flow. Therefore, we need to establish an energy conservation equation. The fluid heat transfer in coiled tubing is shown in Figure 1.

According to the law of energy conservation, the energy equation in the coiled tubing can be obtained.

$$\frac{d}{dz}\left(H_m - gz + \frac{v^2}{2}\right) + \frac{1}{w}\frac{Q_{\mathrm{ct}}}{dz} + \frac{1}{w}\frac{Q_{\mathrm{Frg}}}{dz} = 0. \quad (1)$$

Similarly, we can obtain the energy equation within the annulus of the coiled tubing.

$$\frac{d}{dz}\left(H_m + gz + \frac{v^2}{2}\right) + \frac{1}{w}\frac{Q_a}{dz} - \frac{1}{w}\frac{Q_{\mathrm{ct}}}{dz} + \frac{1}{w}\frac{Q_{\mathrm{Fra}}}{dz} = 0. \quad (2)$$

Due to the enthalpy as a function of pressure and temperature, there is the following expression:

$$dH_m = \left(\frac{\partial H_m}{\partial T}\right)_p dT + \left(\frac{\partial H_m}{\partial p}\right)_T dp = c_p dT - c_p \mu_J dp. \quad (3)$$

Substituting equation (3) into equations (1) and (2), we can obtain the following:

$$c_{\mathrm{pg}}\frac{dT_g}{dz} - c_{pg}\mu_J\frac{dp_g}{dz} - g + v_g\frac{dv_g}{dz} + \frac{Q_{\mathrm{ct}}}{w_g dz} + \frac{Q_{\mathrm{Frg}}}{w_g dz} = 0, \quad (4)$$

$$c_{\mathrm{pa}}\frac{dT_a}{dz} - c_{\mathrm{pa}}\mu_J\frac{dp_a}{dz} + g + v_a\frac{dv_a}{dz} + \frac{Q_a}{w_a dz} - \frac{Q_{\mathrm{ct}}}{w_a dz} + \frac{Q_{\mathrm{Fra}}}{w_a dz} = 0. \quad (5)$$

The next step is to express the terms in Eq. (4) and Eq. (5).

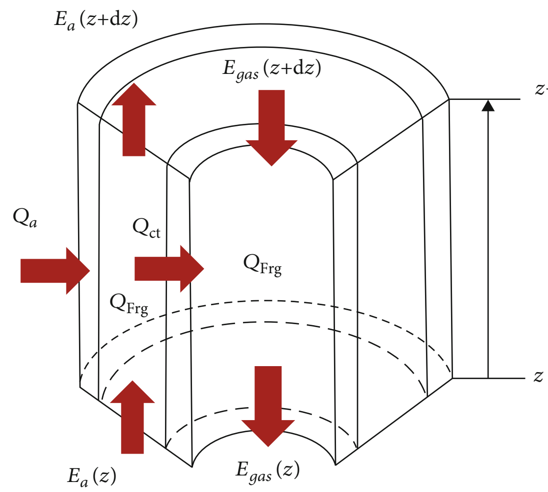

Figure 1: Coiled tubing gas lift wellbore heat transfer process.

(a) Total radial heat transfer from formation to coiled tubing annulus:

Expression for heat transfer between well wall and coiled tubing annulus:

$$Q_{\mathrm{wa}} = 2\pi r_{\mathrm{ti}} U_a (T_{\mathrm{wb}} - T_a) dz. \quad (6)$$

Expression for heat transfer between formation and well wall:

$$Q_{\mathrm{ew}} = \frac{2\pi k_e (T_e - T_{\mathrm{wb}})}{f(t_D)} dz. \quad (7)$$

$f(t_D)$ is the transient heat transfer function, which is calculated as follows [5]:

$$\begin{cases} f(t_D) = 1.1281\sqrt{t_D}\left(1 - 0.3\sqrt{t_D}\right) & 10^{-10} \le t_D \le 1.5 \\ f(t_D) = [0.4036 + 0.5\ln(t_D)]\left(1 + \dfrac{0.6}{t_D}\right) & t_D > 1.5 \end{cases}. \quad (8)$$

The total radial heat transfer from the formation to the coiled tubing annulus can be obtained by equating equations (6) and (7):

$$Q_a = \frac{2\pi r_{\mathrm{ti}} k_e U_a}{k_e + r_{\mathrm{ti}} U_a f(t_D)} (T_e - T_a) dz. \quad (9)$$

(b) Total radial heat transfer from seawater to coiled tubing annulus:

$$Q_a = 2\pi r_{\mathrm{ti}} U_a (T_e - T_a) dz. \tag{10}$$

(c) Total heat transfer from the coiled tubing annulus to the interior of the coiled tubing:

$$Q_{\mathrm{ct}} = 2\pi r_{\mathrm{lti}} U_{\mathrm{ct}} (T_a - T_g) dz. \tag{11}$$

(d) Friction heat between fluid and pipe wall:

Coiled tubing interior:

$$Q_{\mathrm{Frg}} = \frac{w_g \lambda_g v_g^2}{4 r_{\mathrm{lti}}} dz. \tag{12}$$

Coiled tubing annulus:

$$Q_{\mathrm{Fra}} = \frac{w_a \lambda_a v_a^2}{4 r_a} dz. \tag{13}$$

Substitute Eqs. (9)–Eqs. (13) into Eq. (4) and Eq. (5) to obtain the differential equation of wellbore temperature inside the coiled tubing:

$$\frac{dT_g}{dz} = \mu_J \frac{dp_g}{dz} + \frac{1}{c_{\mathrm{pg}}} \left(g - v_g \frac{dv_g}{dz} - \frac{\lambda_g v_g^2}{4 r_{\mathrm{lti}}} \right) - D_1 (T_a - T_g). \tag{14}$$

Similarly, we can obtain the wellbore temperature differential equation for the coiled tubing annulus:

$$\begin{aligned} \frac{dT_a}{dz} = \mu_J \frac{dp_a}{dz} - \frac{1}{c_{\mathrm{pa}}} \left(g + v_a \frac{dv_a}{dz} + \frac{\lambda_a v_a^2}{4 r_a} \right) \\ + D_2 (T_a - T_g) - E(T_e - T_a), \end{aligned} \tag{15}$$

where

$$\begin{aligned} D_1 &= \frac{2\pi r_{\mathrm{lti}} U_{\mathrm{ct}}}{w_g c_{\mathrm{pg}}}, \\ D_2 &= \frac{2\pi r_{\mathrm{lti}} U_{\mathrm{ct}}}{w_{\mathrm{a}} c_{\mathrm{pa}}}, \end{aligned} \tag{16}$$

formation:

$$E = \frac{2\pi r_{\mathrm{ti}} k_e U_a}{w_a c_{\mathrm{pa}} [k_e + r_{\mathrm{ti}} U_a f(t_D)]}. \tag{17}$$

Seawater:

$$E = \frac{2\pi r_{\mathrm{ti}} U_a}{w_a c_{\mathrm{pa}}}. \tag{18}$$

Some heat transfer parameters of the differential equation are interrelated, and it is difficult to obtain analytical expression, so it needs to be solved by the difference numerical method. The entire wellbore is meshed as shown in Figure 2.

The differential equation of wellbore temperature in coiled tubing has been processed by the finite difference method as follows:

$$\begin{aligned} \frac{T_g^{n+1} - T_g^n}{\Delta z} &= \mu_J \left(\frac{p_g^{n+1} - p_g^n}{\Delta z} \right) \\ &\quad + \frac{1}{c_{\mathrm{pg}}} \left[g - \left(v_g^n \frac{v_g^{n+1} - v_g^n}{\Delta z} \right) - \frac{\lambda_g v_g^{2n}}{4 r_{\mathrm{lti}}} \right] - D_1 \left(T_a^n - T_g^n \right). \end{aligned} \tag{19}$$

Similarly, the wellbore temperature differential equation after finite difference treatment of the coiled tubing annulus can be obtained:

$$\begin{aligned} \frac{T_a^{n+1} - T_a^n}{\Delta z} &= \mu_J \left(\frac{p_a^{n+1} - p_a^n}{\Delta z} \right) \\ &\quad - \frac{1}{c_{\mathrm{pa}}} \left[g + \left(v_a^n \frac{v_a^{n+1} - v_a^n}{\Delta z} \right) + \frac{\lambda_a v_a^{2n}}{4 r_a} \right] \\ &\quad - D_2 \left(T_a^n - T_g^n \right) + E(T_e^n - T_a^n). \end{aligned} \tag{20}$$

After simplification, the temperature calculation formulas for the inner and annular of the coiled tubing can be obtained:

$$\begin{aligned} T_g^{n+1} &= T_g^n + \mu_J \left(p_g^{n+1} - p_g^n \right) \\ &\quad + \frac{1}{c_{\mathrm{pg}}} \left[g\Delta z - v_g^n \left(v_g^{n+1} - v_g^n \right) - \frac{\lambda_g v_g^{2n} \Delta z}{4 r_{\mathrm{lti}}} \right] - D_1 \left(T_a^n - T_g^n \right) \Delta z, \\ T_a^{n+1} &= T_a^n + \mu_J (p_a^{n+1} - p_a^n) \\ &\quad - \frac{1}{c_{\mathrm{pa}}} \left[g\Delta z + v_a^n (v_a^{n+1} - v_a^n) + \frac{\lambda_a v_a^{2n} \Delta z}{4 r_a} \right] \\ &\quad - D_2 \left(T_a^n - T_g^n \right) \Delta z + E(T_e^n - T_a^n) \Delta z. \end{aligned} \tag{21}$$

The temperature T_m expression for the mixture of gas and liquid injected at the bottom of the coiled tubing is

$$c_{\mathrm{pg}} w_g T_g + c_{pf} w_f T_f = c_{\mathrm{pm}} w_m T_m. \tag{22}$$

2.3. Calculation of Heat Transfer Coefficient. The coiled tubing is located inside the tubing, and the fluid heat transfer process in the formation section includes gas convection heat transfer, coiled tubing wall heat transfer, coiled tubing and tubing annulus fluid convection heat transfer, tubing wall heat transfer, oil sleeve annulus composite heat transfer, casing wall heat transfer, cement sheath heat transfer, and formation heat transfer from the inside out. The heat transfer in the seawater section is different from that in the formation section, only gas convection heat transfer, coiled

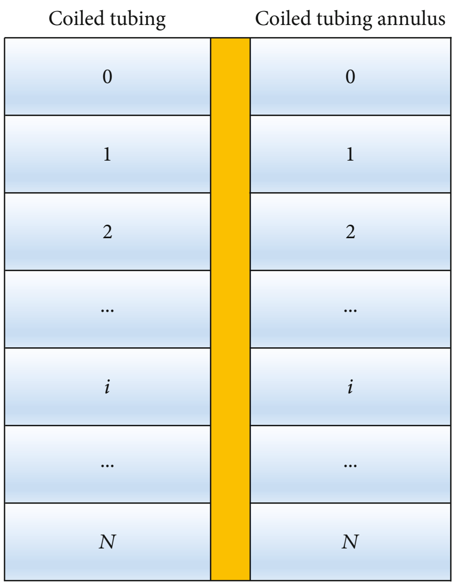

FIGURE 2: Coiled tubing and coiled tubing annular grid structure division.

tubing wall heat transfer, fluid convection heat transfer between coiled tubing and tubing annulus, tubing wall heat transfer, tubing and riser annulus heat transfer, riser wall heat transfer, and seawater heat transfer. The radial heat transfer situation of the wellbore in the coiled tubing gas lift formation section and seawater section is shown in Figure 3.

Using the principle of thermal resistance series connection, the total thermal resistance of the wellbore in the formation section and seawater section is calculated, and then, the total heat transfer coefficient is obtained.

(a) Formation section:

$$\begin{aligned}R_a &= \frac{1}{2\pi}\left(\frac{1}{r_{\mathrm{ti}}h_{\mathrm{lfa}}} + \frac{1}{\lambda_{\mathrm{tub}}}\ln\frac{r_{\mathrm{to}}}{r_{\mathrm{ti}}} + \frac{1}{r_{\mathrm{ci}}(h_c+h_r)} + \frac{1}{\lambda_{\mathrm{cas}}}\ln\frac{r_{\mathrm{co}}}{r_{\mathrm{ci}}} + \frac{1}{\lambda_{\mathrm{cem}}}\ln\frac{r_{\mathrm{cem}}}{r_{\mathrm{co}}}\right),\\ U_a &= \left(\frac{1}{h_{\mathrm{lfa}}} + \frac{r_{\mathrm{ti}}}{\lambda_{\mathrm{tub}}}\ln\frac{r_{\mathrm{to}}}{r_{\mathrm{ti}}} + \frac{r_{\mathrm{ti}}}{r_{\mathrm{ci}}(h_c+h_r)} + \frac{r_{\mathrm{ti}}}{\lambda_{\mathrm{cas}}}\ln\frac{r_{\mathrm{co}}}{r_{\mathrm{ci}}} + \frac{r_{\mathrm{ti}}}{\lambda_{\mathrm{cem}}}\ln\frac{r_{\mathrm{cem}}}{r_{\mathrm{co}}}\right)^{-1}.\end{aligned} \tag{23}$$

(b) Seawater section:

$$\begin{aligned}R_a &= \frac{1}{2\pi}\left(\frac{1}{r_{\mathrm{ti}}h_{\mathrm{lfa}}} + \frac{1}{\lambda_{\mathrm{tub}}}\ln\frac{r_{\mathrm{to}}}{r_{\mathrm{ti}}} + \frac{1}{r_{\mathrm{ri}}(h_c+h_r)} + \frac{1}{\lambda_r}\ln\frac{r_{\mathrm{ro}}}{r_{\mathrm{ri}}}\right),\\ U_a &= \left(\frac{1}{h_{\mathrm{lfa}}} + \frac{r_{\mathrm{ti}}}{\lambda_{\mathrm{tub}}}\ln\frac{r_{\mathrm{to}}}{r_{\mathrm{ti}}} + \frac{r_{\mathrm{ti}}}{r_{\mathrm{ri}}(h_c+h_r)} + \frac{r_{\mathrm{ti}}}{\lambda_r}\ln\frac{r_{\mathrm{ro}}}{r_{\mathrm{ri}}}\right)^{-1}.\end{aligned} \tag{24}$$

2.4. Calculation of Pressure. When the formation produced liquid and injected gas flows along the annulus between the coiled tubing and the tubing, the annulus fluid is gas-liquid two-phase. Previous studies have conducted a lot of research on two-phase flow pressure models, which are generally divided into empirical models and mechanism models. The empirical model includes ([18–21]. The empirical model obtains a large amount of data through indoor experiments or on-site production, so the calculation results rely more on the values of experimental and on-site production data. However, the physical parameters of crude oil at different sites vary greatly, which will lead to poor calculation accuracy of the model. The mechanism model is based on the principle of fluid mechanics to establish parameter relations, which can cover all the parameters that affect the multiphase flow law, and the calculation accuracy is high. At present, the model proposed by [22] is one of the commonly used mechanism models. The pressure calculation formula is as follows:

$$-\frac{dp}{dz} = \rho_m g + \frac{2f_m v_m^2 \rho_m}{D} + \rho_m v_m \frac{dv_m}{dz}. \tag{25}$$

2.5. Fluid Property Equation. The density of gas injected into a coiled tubing is calculated using the gas state equation:

$$\rho_g = \frac{\mathrm{PM}}{\mathrm{RT}}. \tag{26}$$

Due to the low compressibility of heavy oil as a liquid, the density calculation formula for heavy oil only considers the influence of temperature [23]:

$$\rho_o = \rho_{20} + (13.561 - 0.191x)\times 10^{-3} - (63.9 - 0.87x)\times 10^{-5}T^{1.02}. \tag{27}$$

The formula for the variation of viscosity of heavy oil with temperature is [24]

$$\lg\lg\mu_o = A - B\lg(T - 273.15). \tag{28}$$

2.6. A Coupled Solution Method for Temperature and Pressure. Coiled tubing gas lift involves complex two-phase flow, with the interaction of fluid temperature, pressure, and physical parameters, resulting in complex calculations. Therefore, it is necessary to couple and solve the wellbore temperature and pressure.

2.6.1. Boundary Condition. When setting the boundary conditions for the coupling calculation, the gas injection temperature $T_{\mathrm{inj},0}$ and pressure $P_{\mathrm{inj},0}$ are known. In addition, we also need to know a set of boundary conditions to solve the model. We assume that the pressure and temperature of the injected gas at the bottom of the coiled tubing are $T_{\mathrm{inj},n}{}'$ and $P_{\mathrm{inj},n}{}'$. Then, use Eq. (22) to find the mixing temperature $T_m{}'$ and $P_m{}'$. Use the assumed boundary conditions to back-calculate the wellhead temperature$T_{\mathrm{inj},0}{}'$ and$P_{\mathrm{inj},0}{}'$pressure under this assumed condition. Compare the difference between $T_{\mathrm{inj},0}{}'$ and $P_{\mathrm{inj},0}{}'$ and $T_{\mathrm{inj},0}$ and $P_{\mathrm{inj},0}$ to determine whether the accuracy requirements are met. If the requirements are met, the assumed boundary

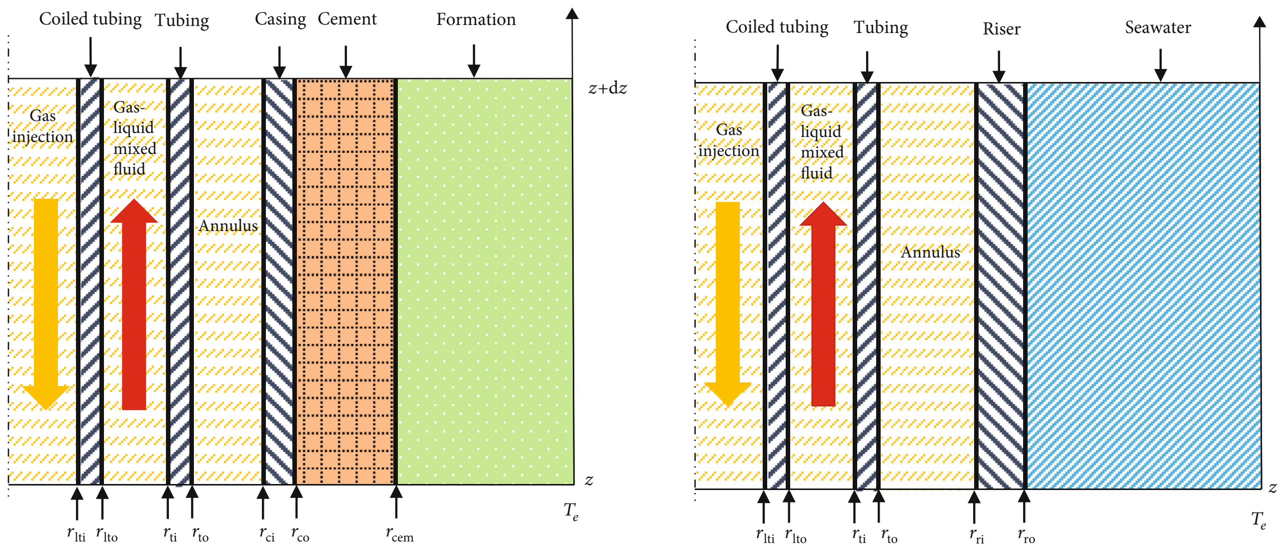

Figure 3: Schematic diagram of radial heat transfer in the wellbore of the coiled tubing gas lift formation section and seawater section.

conditions are correct; otherwise, continue to assume until the accuracy requirements are met.

2.6.2. Calculation Steps for Wellbore Coupled Temperature and Pressure Field

(a) The length of the wellbore is L, divided into n sections, each with a length of $dz = L/n$

(b) Given the boundary temperature T_i and boundary pressure P_i, assuming temperature changes ΔT and pressure changes ΔP. Then, the next temperature is T', and the pressure is P';

(c) Calculate the average temperature $\bar{T}$ and average pressure $\bar{P}$ of the wellbore within the length dz and obtain the thermophysical parameters at this temperature and pressure

(d) Determine the flow pattern characteristics of the section based on the apparent velocity and calculate the heat transfer coefficient and pressure drop gradient for the section

(e) Substitute the relevant parameters into the established temperature and pressure model to obtain the next temperature T_{i+1} and pressure P_{i+1}

(f) Compare the difference between temperature T' and pressure P' and the calculated temperature T_{i+1} and pressure P_{i+1}. If the difference does not meet the calculation accuracy, start from (b) and assume the temperature T' and pressure P' again. Otherwise, continue to calculate the next section until the wellbore calculation is completed

The frame diagram of the program calculation is shown in Figure 4.

3. Analysis of Coiled Tubing Gas Lift Temperature Field

3.1. Offshore Heavy Oil Test Well Basis Parameters and Mobility Analysis. X1 is a heavy oil test well in the South China Sea, the subsea mudline position is 158.5 m, and the total length of the well body is 3643.38 m. The sea surface temperature is 23°C, the submarine mudline temperature is 15°C, the crude oil inflection point temperature is about 33°C, and the temperature in the middle of the reservoir is 134.87°C. X2 represents a deep-water heavy oil test well, the mudline temperature of X2 is about 4.2°C, 1050 m from the wellhead, and the total length of the well body is 4200 m. Other conditions are the same as for well X1. According to known conditions, the temperature and viscosity curves of X1 and X2 with well depth are shown in Figures 5 and 6.

Combining Figures 5 and 6, it can be seen that the temperature of crude oil in well X1 continues to decrease as it flows up the wellbore. This is due to the fact that the crude oil temperature is higher than the ambient temperature and heat loss occurs with flow, and the heat loss of crude oil in the seawater section is greater than that in the formation section. The reason is that the temperature of crude oil is higher than the ambient temperature, causing heat loss as it flows, and the heat loss of crude oil in the seawater section is greater than that in the formation section. However, the crude oil temperature of X2 decreased to a certain extent and began to rise. The reason is that X2 is in a deep-water environment, and when the crude oil drops to the seawater temperature, the environmental temperature is higher than the wellbore, transferring heat to the fluid in the well, resulting in an increase in the heat absorption temperature of the crude oil.

3.2. Influence of Coiled Tubing Running Depth on Temperature Distribution. In order to analyze the influence of the change of coiled tubing running depth on the crude oil temperature and optimize the reasonable string length.

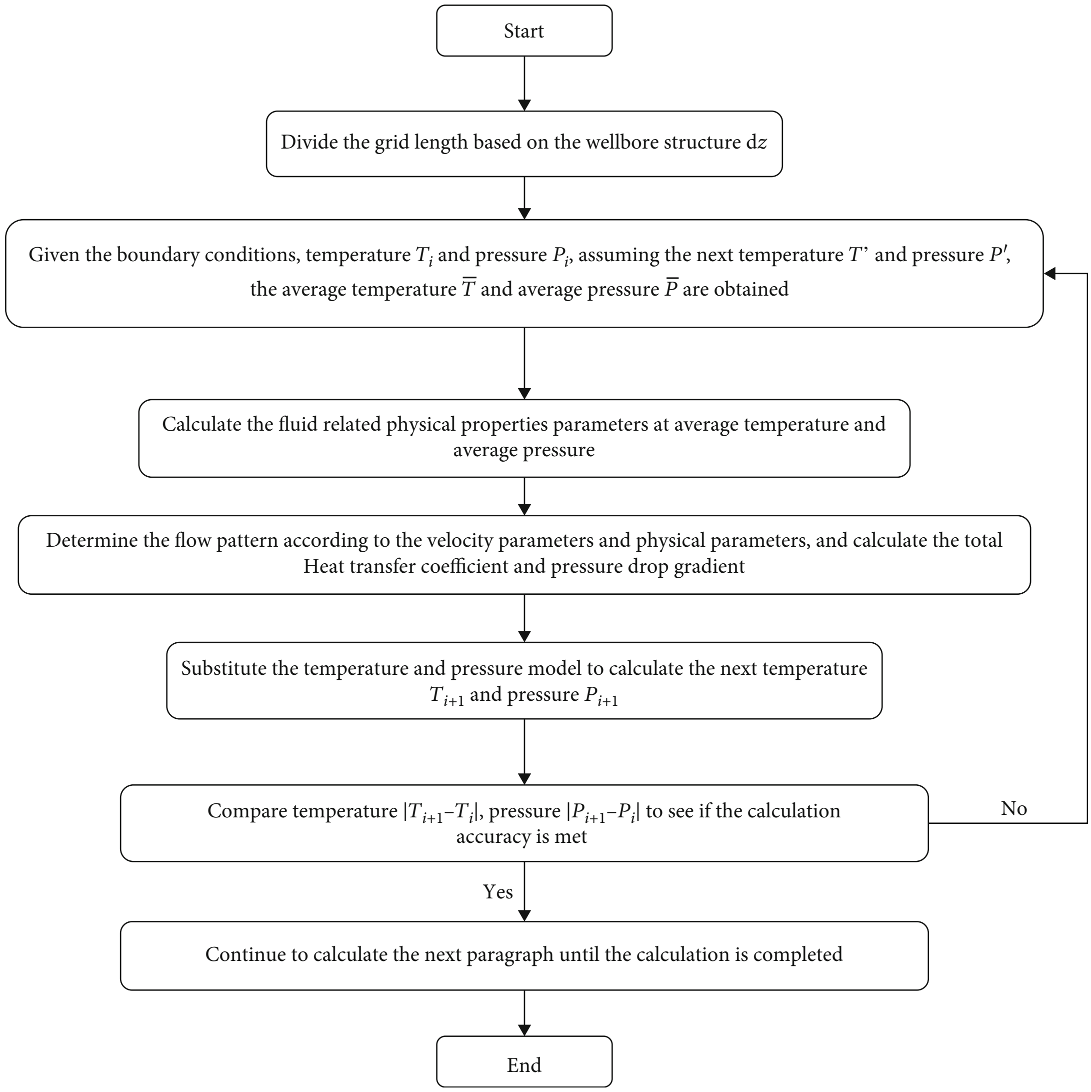

Figure 4: Structure diagram of the coupling calculation program.

Under the conditions of gas injection temperature of 25°C and gas injection rate of 1200 m^3/h, the distribution curves of crude oil temperature with the depth of coiled tubing running were obtained for X1 and X2 wellbores as shown in Figures 7 and 8, respectively.

The following conclusions can be obtained by analyzing the crude oil temperature distribution curve of X1 and X2 with the depth of coiled tubing running. As the depth of coiled tubing increases in X1, the length of the well section where the crude oil temperature is lower than the inflection point temperature changes less. And as the depth of coiled tubing increases in X2, the length of the well section where the crude oil temperature is lower than the inflection point temperature shows a trend of first increasing and then decreasing. The reason for this phenomenon is that the deeper the coiled tubing is lowered, the temperature of the gas mixed with the crude oil is lower than the inflection point temperature, and the length of the coiled tubing at this time is the low-temperature well section below the inflection point temperature. As the running depth of coiled tubing continues to increase, the mixing temperature is higher than the inflection point temperature, and the total heat transfer coefficient in the annulus decreases; the mixing fluid temperature decreases slowly, so the number of well sections below the inflection point temperature decreases. Based on the above analysis results, it can be concluded that when the depth of seawater is shallow, changing the running depth of coiled tubing has little effect on the fluidity of crude oil. However, when the seawater depth is deeper, the length of the well section in which crude oil flows smoothly increases after the length of coiled tubing exceeds a certain running depth.

3.3. Influence of Coiled Tubing Gas Injection Temperature on Temperature Distribution. In order to better observe the wellbore temperature profile characteristics, the running depth of the coiled tubing in X1 and X2 is 1500 m and 2500 m, respectively. The temperature range of gas injection is between 25 and 40°C. The curves of wellbore crude oil

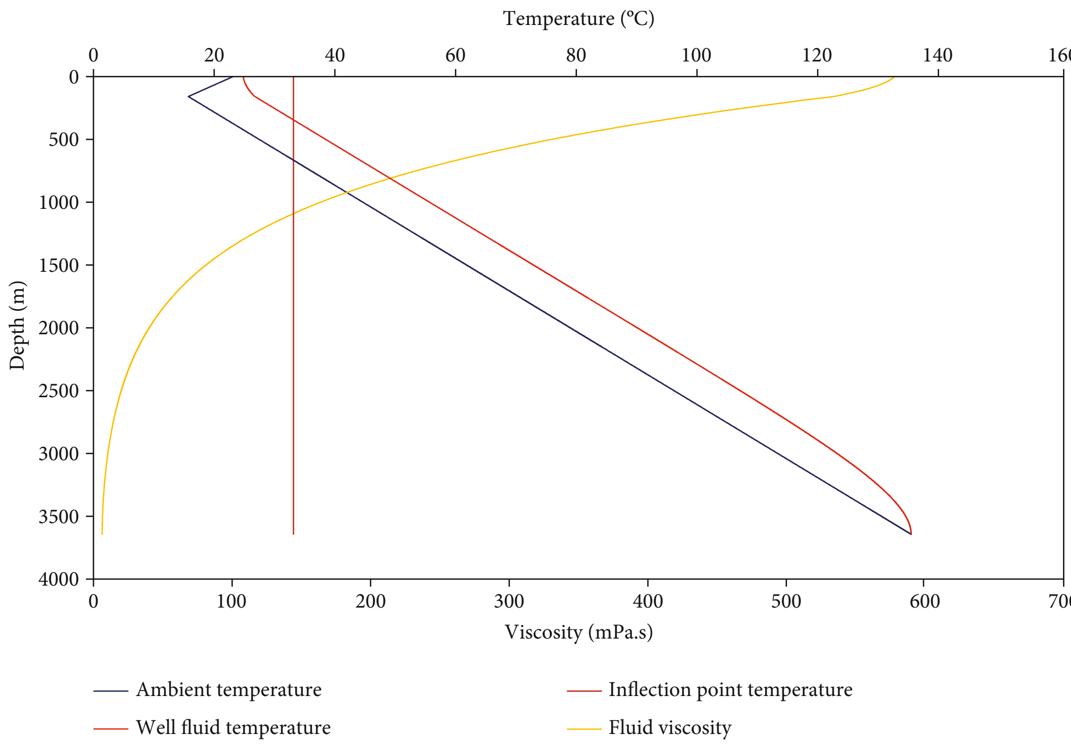

Figure 5: Temperature and viscosity variation curve of crude oil in X1 with well depth.

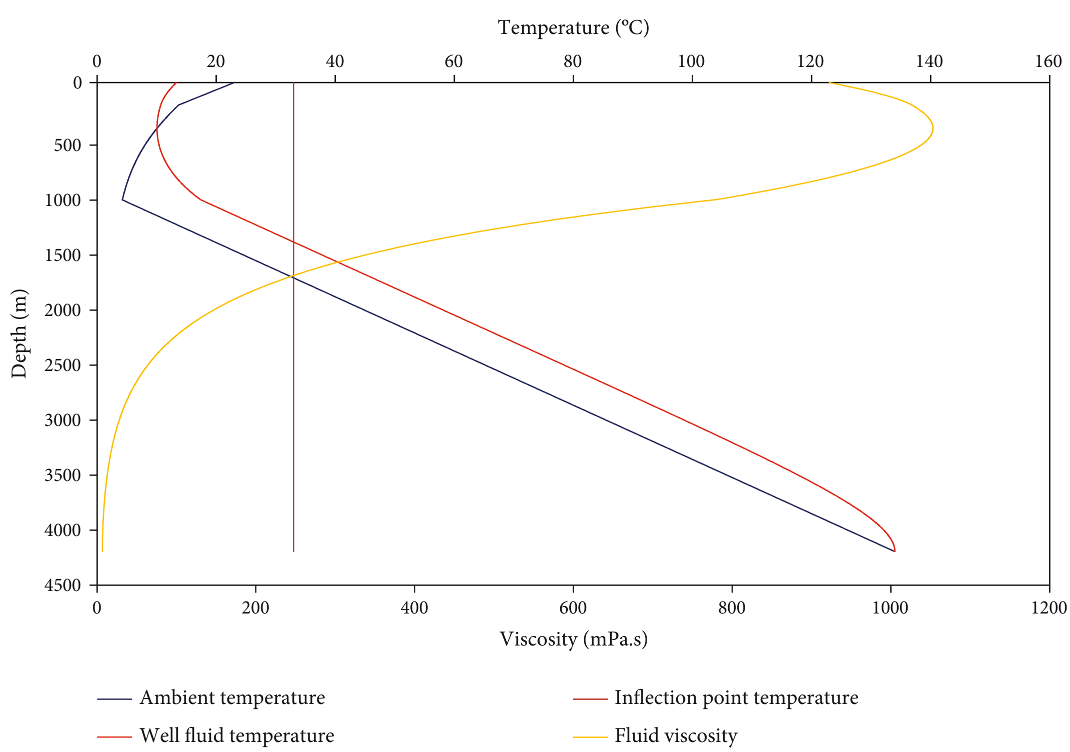

Figure 6: Temperature and viscosity variation curve of crude oil in X2 with well depth.

temperature changing with gas injection temperature are shown in Figures 9 and 10.

As can be seen from Figures 9 and 10, the corresponding mixing temperature at the bottom of the coiled tubing gradually increases as the injected gas temperature increases. For every 5°C increase in injected gas, the average fluid temperature in the annulus of X1 increases by more than 4°C, but X2 only increases by 2-3°C. When the gas injection

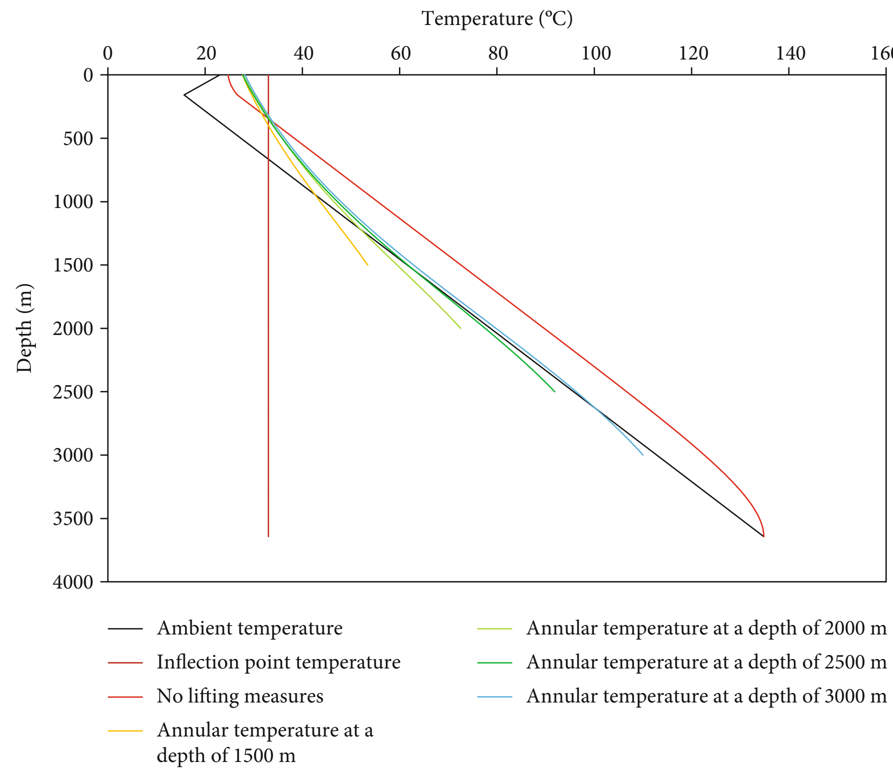

Figure 7: Distribution curve of crude oil temperature with running depth of coiled tubing in X1.

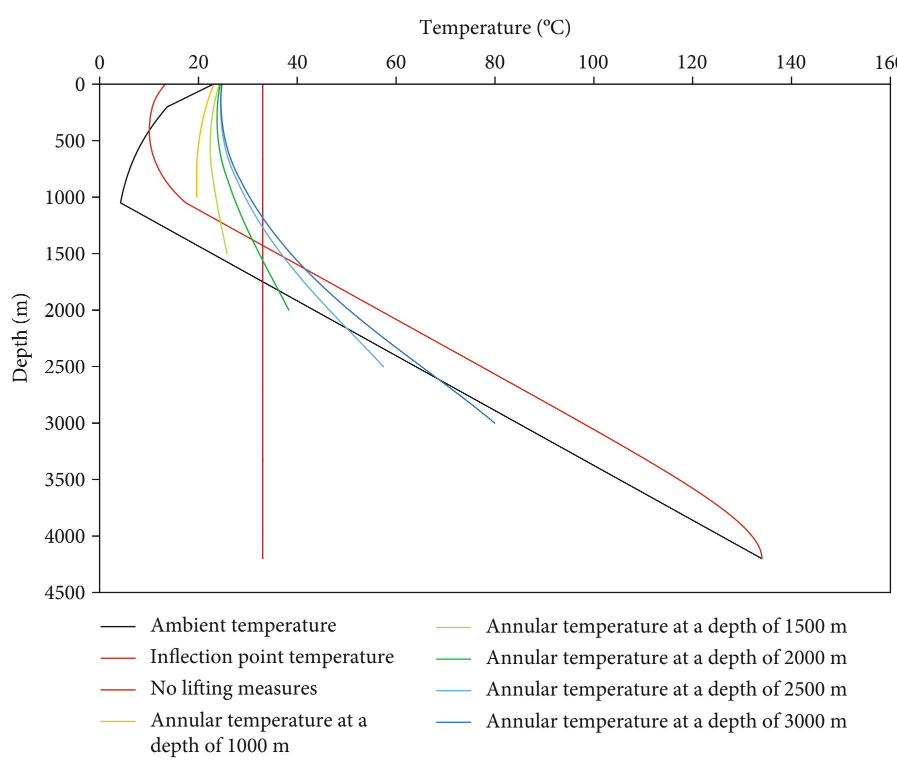

Figure 8: Distribution curve of crude oil temperature with running depth of coiled tubing in X2.

temperature exceeds 30°C, the lowest temperature of X1 annular fluid can reach the inflection point temperature to meet the flow conditions of heavy oil. However, for X2, only when the injection temperature is at least 45°C can the minimum temperature of the annular fluid exceed the inflection point temperature. Based on the above analysis, it can be

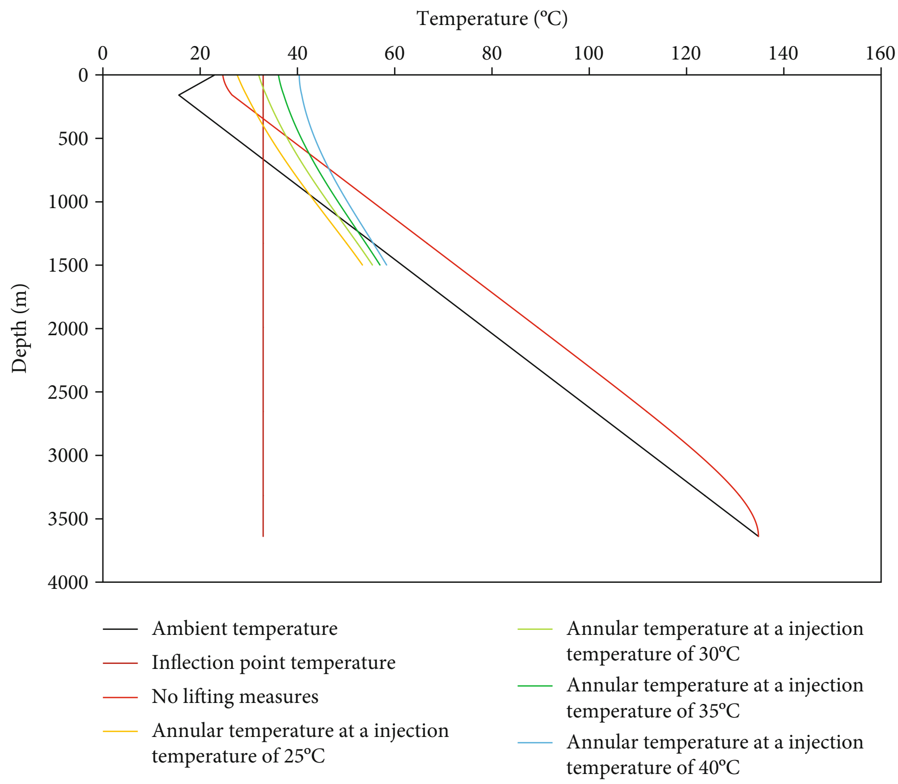

Figure 9: Distribution curve of crude oil temperature with coiled tubing injection temperature in X1.

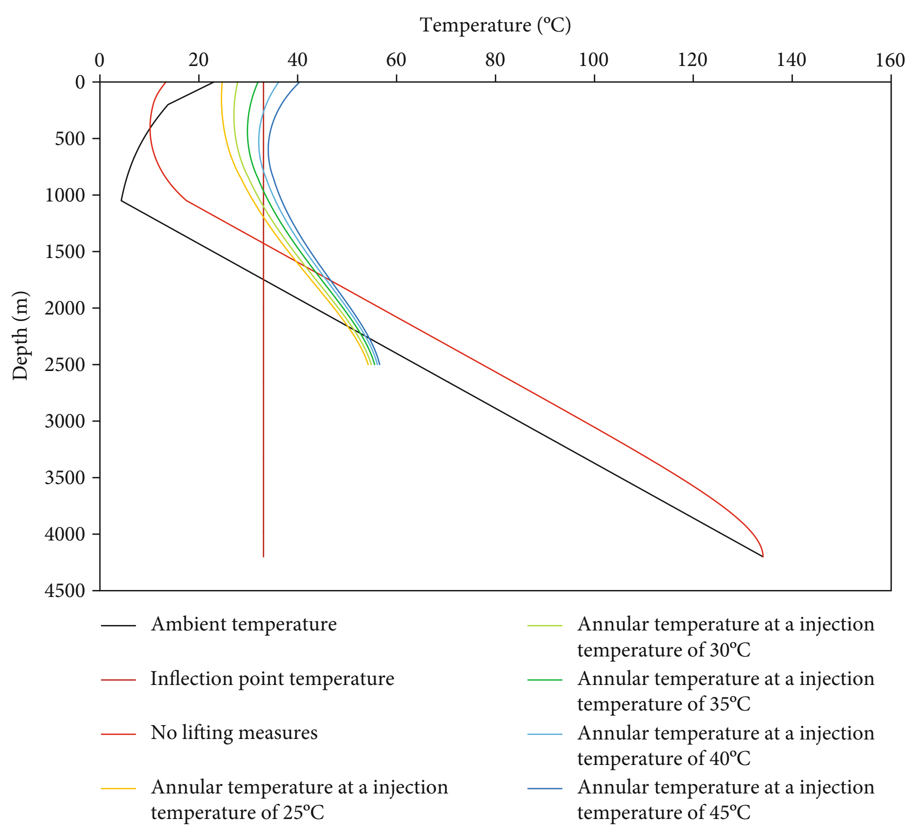

Figure 10: Distribution curve of crude oil temperature with coiled tubing injection temperature in X2.

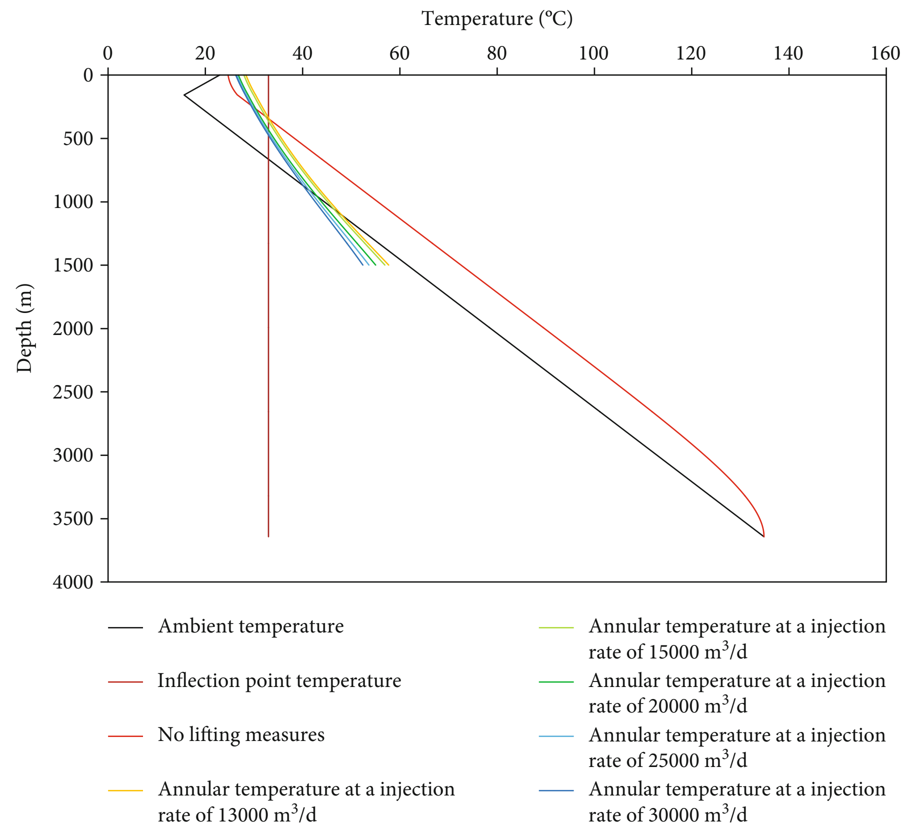

Figure 11: Distribution curve of crude oil temperature with gas injection rate in X1.

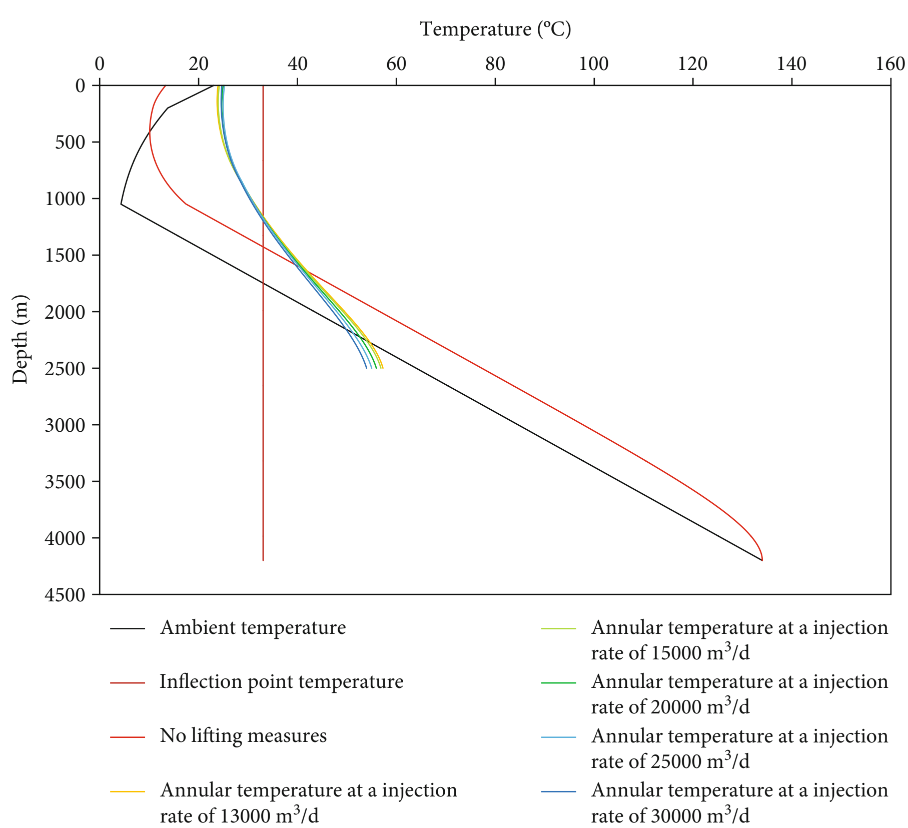

Figure 12: Distribution curve of crude oil temperature with gas injection rate in X2.

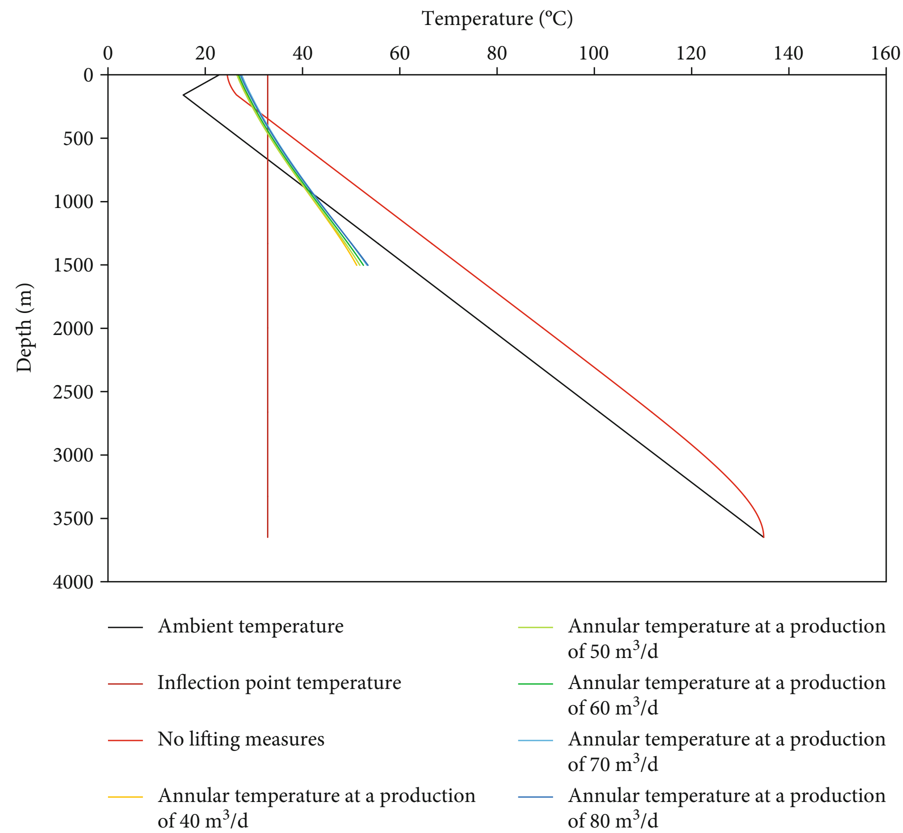

Figure 13: Distribution curve of crude oil temperature with production in X1.

seen that the injection temperature has a significant impact on the temperature of the annular fluid. Therefore, increasing the injection temperature can effectively improve the fluidity of heavy oil.

3.4. Influence of Gas Injection Rate of Coiled Tubing on Temperature Distribution. When studying the influence of coiled tubing gas injection rate on crude oil temperature, the gas injection rate range is between 13000 and 30000 m^3/d. At the same time, other basic parameters need to be kept the same. The curves of wellbore crude oil temperature changing with gas injection rate are shown in Figures 11 and 12.

From the calculation results, it can be seen that there are slight differences in the trend of crude oil temperature changes between the two wells when changing the gas injection rate of the coiled tubing. As the gas injection rate increases, the crude oil temperature at the wellhead of X1 will slightly decrease, while the crude oil temperature at the wellhead of X2 will first increase and then decrease. Analysis suggests that a large injection rate of gas into X1 will cause slow gas temperature rise in the coiled tubing, lower mixing temperature, and lower crude oil temperature. The seawater in X2 is relatively deep, and the low temperature section has a significant impact on the flow of crude oil. An increase in initial gas flow rate will result in an increase in flow rate, a reduction in heat loss between the gas-liquid mixture and the environment, and an increase in temperature near the wellhead. But as the gas injection rate continues to increase, the heat that decreases in the mixing temperature is greater than the heat retained due to the fast flow rate. The increase in coiled tubing gas injection rate increases the number of well sections with crude oil temperatures below the inflection point temperature. Therefore, there may be a dampening effect on crude oil warming after a certain amount of gas injection is reached.

3.5. Influence of Crude Oil Production on Temperature Distribution. When studying the influence of crude oil production on temperature, the crude oil production range is between 40 and 80 m^3/d. At the same time, other basic parameters need to be kept the same. The curves of wellbore crude oil temperature changing with production are shown in Figures 13 and 14.

It can be seen from the calculation results that the crude oil temperature at the wellhead has increased in both X1 and X2 compared with that without lifting, but with the increase of production, the crude oil temperature distribution curve almost coincides. Therefore, under conditions of high gas injection rate, increasing a small amount of production has almost no effect on the temperature of the annular fluid. Analysis shows that although production has been constantly changing, there is a significant difference in the ratio of gas injection to production. The entire annulus is dominated by gas phase, and a small increase or decrease in

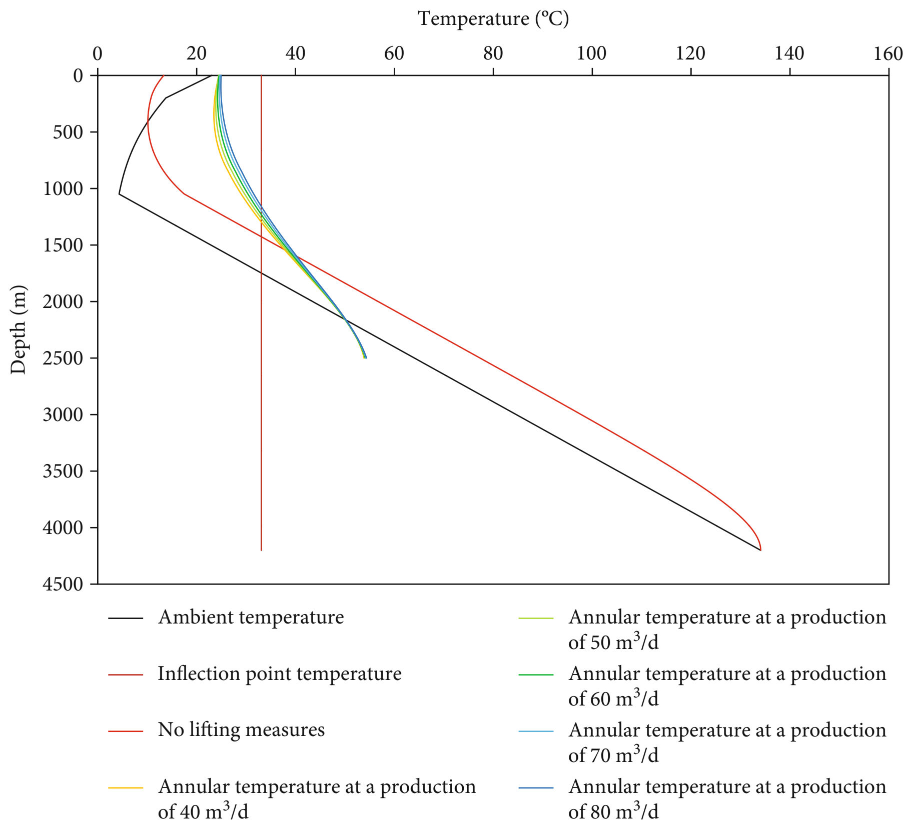

FIGURE 14: Distribution curve of crude oil temperature with production in X2.

production has very little impact on the temperature of the annular crude oil. Therefore, crude oil production has little influence on wellbore temperature distribution.

3.6. Influence of Coiled Tubing Diameter on Temperature Distribution. When studying the influence of coiled tubing diameter on temperature, the coiled tubing diameter range is between 31.8 and 50.8 mm. At the same time, other basic parameters need to be kept the same. The curves of wellbore crude oil temperature changing with coiled tubing diameter are shown in Figures 15 and 16.

From the calculation results, it can be seen that as the diameter of the coiled tubing increases, the fluid temperature at the mixing position keeps increasing. After the fluid flows upwards along the wellbore to a certain depth in the well, the temperature of the larger diameter fluid begins to be lower than that of the smaller diameter fluid. It is analyzed that as the diameter of the coiled oil pipe increases, the flow rate of the injected gas in the coiled oil pipe decreases, and the lower temperature-injected gas exchanges more heat with the annular fluid and reaches a higher temperature at the bottom of the coiled tube. During the process of mixed fluid returning in the annulus, there is a significant heat exchange between the mixed fluid and the external environment and the injected gas from the coiled tubing, resulting in a faster decrease in the temperature of the annulus fluid with a larger diameter of the coiled tubing compared to the annulus fluid with a smaller diameter. Increasing the diameter of the coiled tubing results in smaller changes in the length of the well section where the crude oil temperature is lower than the inflection point temperature, resulting in poor effectiveness in improving flowability.

3.7. Evaluation of Lifting Parameters. Based on the above analysis, it can be seen that when X1 and X2 were subjected to the coiled tubing gas lift process, changing the lift parameters affected the crude oil temperature and fluidity of both wells to different degrees. A comprehensive comparison reveals that the injection temperature of the coiled tubing has the greatest impact on the crude oil temperature when coiled tubing is used for gas injection compared to unassisted measures. After increasing the injection temperature of coiled tubing, the minimum temperature of wellbore crude oil can exceed the inflection point temperature, effectively improving wellbore flow. Although parameters such as crude oil production, coiled tubing depth, gas injection rate, and coiled tubing diameter have, to some extent, improved the minimum temperature of crude oil, the length of well sections below the inflection point temperature has little variation, which cannot guarantee the smooth flow of heavy oil underground. Therefore, when formulating a coiled tubing gas lift lifting plan, the main design parameter should be the injection temperature to reduce resource waste such as equipment and materials.

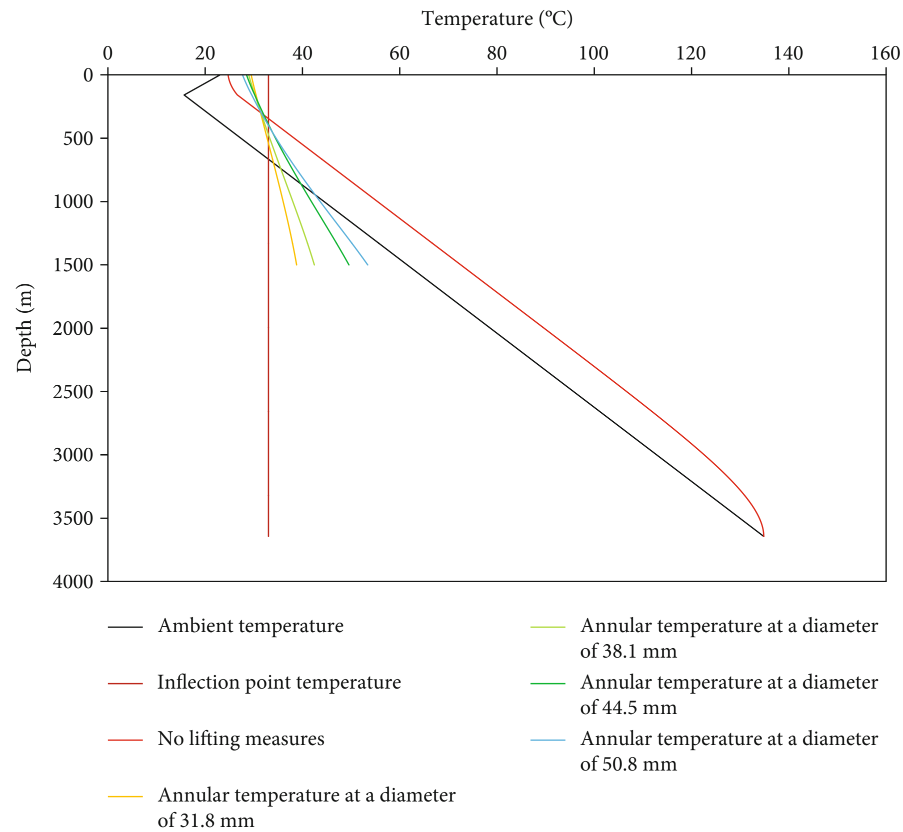

Figure 15: Distribution curve of crude oil temperature with coiled tubing diameter in X1.

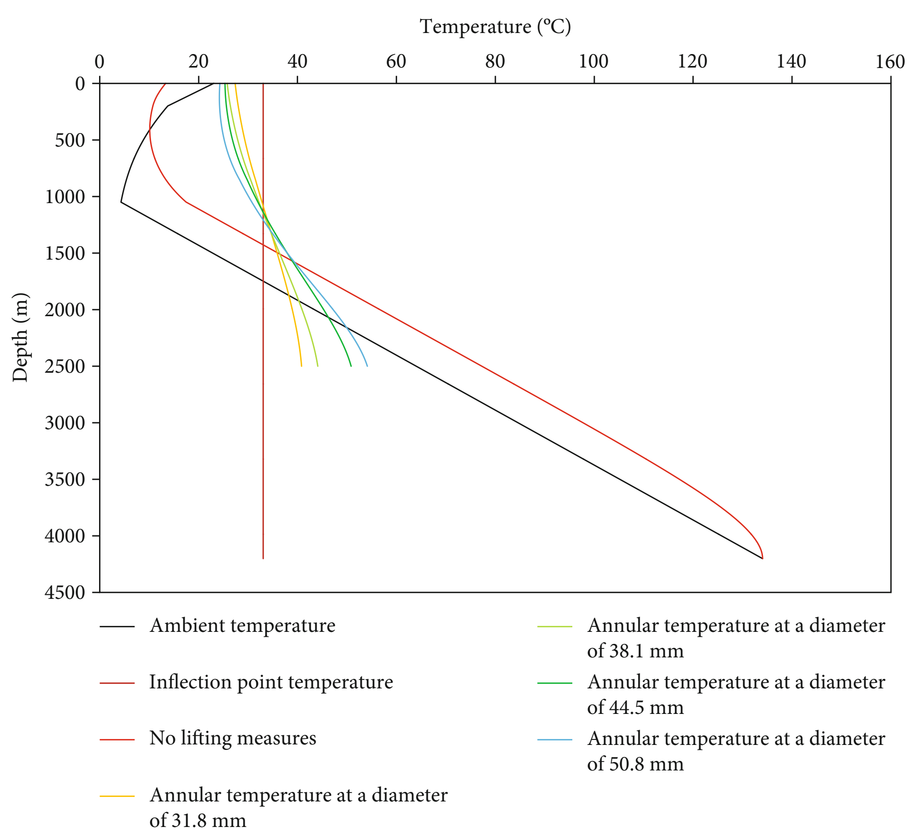

Figure 16: Distribution curve of crude oil temperature with coiled tubing diameter in X2.

4. Conclusion

In this paper, the sensitivity analysis of the factors affecting the temperature distribution of offshore heavy oil wellbore with coiled tubing gas lift is carried out by using the established model. The influence of coiled tubing running depth, gas injection temperature, gas injection rate, diameter, and crude oil production on wellbore temperature distribution is mainly studied. Finally, various lifting parameters of the process were evaluated, and suggestions for optimizing the design of lifting parameters were given. Through the research in this article, the wellbore temperature distribution of offshore heavy oil lifting assisted by coiled tubing gas lift was obtained in both deep and shallow water conditions.

(1) Increasing the depth of coiled tubing penetration has little effect on the crude oil flowability of shallow well; but for deep-water well, when the length of the coiled tubing exceeds a certain depth, the well section where crude oil flows smoothly will increase

(2) Increasing the injection temperature of coiled tubing significantly increases the temperature of both shallow well and deep-water well. Therefore, increasing the injection temperature can effectively improve the fluidity of heavy oil

(3) Increasing the gas injection rate into the coiled tubing will result in a slight decrease in wellhead temperature for shallow well, while for deep-water well, it will first increase and then decrease. Once the gas injection rate reaches a certain value, it will have an inhibitory effect on the increase in crude oil temperature

(4) Increasing crude oil production did not result in a significant increase in crude oil temperature for both shallow well and deep-water well, and changing crude oil production had little effect on the length of the well section below the inflection point temperature, which did not achieve the effect of improving flow

(5) Increasing the diameter of the coiled tubing results in smaller changes in the length of the well section where the crude oil temperature of shallow well and deep-water well is lower than the inflection point temperature, resulting in poor effectiveness in improving flowability

(6) In the coiled tube gas lift lifting offshore heavy oil process, the injection temperature of the coiled tubing has the greatest impact on the crude oil temperature. When designing parameters for this process, the injection temperature should be the main design parameter

Nomenclature

A: Determined by experiments, dimensionless
B: Determined by experiments, dimensionless
c_p: Specific heat capacity of fluid (J/(kg·°C))
c_{pf}: Specific heat capacity of formation fluid at mixing position (J/(kg·°C))
c_{pg}: Specific heat capacity of injection gas at mixing position (J/(kg·°C))
c_{pm}: Heat capacity of two phases at mixing position (J/(kg·°C))
$E_a(z)$: Energy flowing into the bottom of the microelement (J/s)
$E_a(z+dz)$: Energy flowing out of the top of the microelement (J/s)
$E_{\mathrm{gas}}(z+dz)$: Energy of gas flowing into the top of the microelement (J/s)
$E_{\mathrm{gas}}(z)$: Energy of gas flowing out of the bottom of the microelement (J/s)
H_m: Fluid enthalpy (J/kg)
M: Molar mass of injected gas (g/mol)
P: Wellbore pressure (Pa)
Q_a: Heat transfer from the formation (seawater) to the coiled tubing annulus (J/s)
Q_{ct}: Heat transfer from the coiled tubing annulus to the inside of the coiled tubing (J/s)
Q_{Frg}: Friction heat between gas and pipe wall in coiled tubing (J/s)
Q_{Fra}: Friction heat between annular fluid and pipe wall in coiled tubing (J/s)
R: Gas universal constant (J/(mol·°C))
r_a: Equivalent inner diameter of coiled tubing annulus (m)
r_{lti}: Inner diameter of coiled tubing (m)
T: Wellbore temperature (°C)
T_{a}: Fluid temperature in coiled tubing annulus (°C)
T_f: Temperature of formation fluid at the mixing position (°C)
T_g: Coiled tubing gas temperature (°C)
T_m: Mixing position two-phase temperature (°C)
U_a: Total heat transfer coefficient between environment and coiled tubing annulus (W/(m^2·°C))
U_{ct}: Heat transfer coefficient between coiled tubing annulus and coiled tubing (W/(m^2·°C))
w_g: Mass flow rate of injected gas at the mixing position (kg/s)
w_f: Mass flow rate of formation fluid at mixing position (kg/s)
w_{pm}: Mixing position two-phase mass flow rate (kg/s)
x: Coefficient related to surface crude oil density, dimensionless
λ_g: Friction coefficient between gas and pipe wall in coiled tubing, dimensionless
λ_a: Friction coefficient between annular fluid and pipe wall in coiled tubing, dimensionless
μ_o: Viscosity of heavy oil (Pa.s)
μ_{J}: Joule-Thompsoon coefficient
ρ_{20}: Density of heavy oil at 20°C (kg/m^3)
ρ_g: Density of injected gas (kg/m^3)
ρ_o: Density of heavy oil (kg/m^3).

Data Availability

The data used to support the findings of this study are included within the article and available from the corresponding author upon request.

Conflicts of Interest

The authors declare that they have no known competing financial interests or personal relationships that could have appeared to influence the work reported in this paper.

Acknowledgments

The author is very grateful for the support from the CNOOC Science and Technology Project (KJGG2022-0406) and the National Natural Science Foundation of China (Nos. U21B2065 and 52274022).

References

[1] Z. Liu, H. Wang, G. Blackbourn et al., "Heavy oils and oil sands: global distribution and resource assessment," *Acta Geologica Sinica-English Edition*, vol. 93, no. 1, pp. 199–212, 2019.

[2] T. Xiaoguang, G. Zhang, W. Zhaoming et al., "Distribution and potential of global oil and gas resources," *Petroleum Exploration Development*, vol. 45, no. 4, pp. 779–789, 2018.

[3] Y. Liu, H. Yang, L. Zhao et al., "Improve offshore heavy oil recovery by compound stimulation technology involved thermal, gas and chemical methods," in *In Offshore technology conference*, OnePetro, 2010.

[4] A. Khalid, N. Molero, G. Hassan, E. Lovie, and R. S. A. Khan, "Coiled tubing gas lift: an innovative solution for reviving dead wells in southern Pakistan," in *In international petroleum technology conference, D013S110R002*, IPTC, 2020.

[5] A. R. Hasan and C. Kabir, "Aspects of wellbore heat transfer during two-phase flow," *SPE Production & Facilities*, vol. 9, no. 3, pp. 211–216, 1994.

[6] A. R. Hasan, C. S. Kabir, and D. Lin, "Analytic wellbore-temperature model for transient gas-well testing," *SPE Reservoir Evaluation*, vol. 8, no. 3, pp. 240–247, 2005.

[7] A. R. Hasan, C. S. Kabir, and X. Wang, "A robust steady-state model for flowing-fluid temperature in complex wells," *SPE Production*, vol. 24, no. 2, pp. 269–276, 2009.

[8] S. Livescu, L. J. Durlofsky, and K. Aziz, "A semianalytical thermal multiphase wellbore-flow model for use in reservoir simulation," *SPE Journal*, vol. 15, no. 3, pp. 794–804, 2010.

[9] X. Liu, L. Liu, Z. Yu et al., "Study on the coupling model of wellbore temperature and pressure during the production of high temperature and high pressure gas well," *Energy Reports*, vol. 8, pp. 1249–1257, 2022.

[10] H. Liu, Z. Wang, Q. Sun, X. Sun, Y. Liao, and B. Sun, "An improved thermal model for predicting wellbore temperature distribution in deep-water gas well," *Applied Thermal Engineering*, vol. 205, p. 118029, 2022.

[11] M. A. Carrizales, L. W. Lake, and R. T. Johns, "Production improvement of heavy-oil recovery by using electromagnetic heating," in *In SPE Annual Technical Conference and Exhibition*, SPE-115723-MS. SPE, 2008.

[12] Y. Yu, T. Lin, H. Xie, Y. Guan, and K. Li, "Prediction of wellbore temperature profiles during heavy oil production assisted with light oil," in *In SPE Oklahoma City Oil and Gas Symposium/Production and Operations Symposium*, SPE-119526-MS. SPE, 2009.

[13] M. Zhu, H. Zhong, Y. Li, C. Zeng, and Y. Gao, "Research on viscosity-reduction technology by electric heating and blending light oil in ultra-deep heavy oil wells," *Journal of Petroleum Exploration Production Technology*, vol. 5, no. 3, pp. 233–239, 2015.

[14] Y. Kang, Z. Liu, A. Gonzales, and R. Samuel, "Investigating the influence of ESP on wellbore temperature, pressure, annular pressure buildup, and wellbore integrity," in *In SPE Deepwater Drilling and Completions Conference*, OnePetro, 2016.

[15] H. Zhong, S. Zhu, W. Zeng, X. Wang, and F. Zhang, "Research on heavy oil gas lift assisted with light oil injected from the annulus," *Journal of Petroleum Exploration Production Technology*, vol. 8, no. 4, pp. 1465–1471, 2018.

[16] A. R. Hasan and M. Jang, "An analytic model for computing the countercurrent flow of heat in tubing and annulus system and its application: jet pump," *Journal of Petroleum Science Engineering*, vol. 203, p. 108492, 2021.

[17] I. K. Edy, D. N. Wicaksono, R. Saputra, and F. Anantokusumo, "Coiled tubing gas lift design and troubleshooting-case history," in *In SPE Asia Pacific Oil and Gas Conference and Exhibition*, SPE-176195-MS. SPE, 2015.

[18] D. H. Beggs and J. P. Brill, "A study of two-phase flow in inclined pipes," *Journal of Petroleum Technology*, vol. 25, no. 5, pp. 607–617, 1973.

[19] A. R. Hagedorn and K. E. Brown, "Experimental study of pressure gradients occurring during continuous two-phase flow in small-diameter vertical conduits," *Journal of Petroleum Technology*, vol. 17, no. 4, pp. 475–484, 1965.

[20] H. Mukherjee and J. Brill, "Pressure drop correlations for inclined two-phase flow," *Journal of Energy Resources Technology*, vol. 107, no. 4, pp. 549–554, 1985.

[21] J. Orkiszewski, "Predicting two-phase pressure drops in vertical pipe," *Journal of Petroleum Technology*, vol. 19, no. 6, pp. 829–838, 1967.

[22] A. R. Hasan and C. S. Kabir, "A study of multiphase flow behavior in vertical wells," *SPE Production Engineering*, vol. 3, no. 2, pp. 263–272, 1988.

[23] Z. Kang, "General expression of density and temperature of crude oil," *Petroleum Exploration Development*, vol. 26, pp. 107–109, 1999.

[24] Z. Guanghai, L. Zhangcong, X. Xudong, S. Xuncheng, W. Junheng, and W. Bo, "Numerical calculation method of the wellbore temperature field for electric heating heavy oil thermal recovery," *Petroleum Drilling Techniques*, vol. 47, pp. 110–115, 2019.